Aalborg Universitet

AALBORG UNIVERSITY
DENMARK

A Frequency Independent Technique to Estimate Harmonics and Interharmonics in Shipboard Microgrids

Terriche, Yacine; Laib, Abderrzak ; Lashab, Abderezak; Su, Chun-Lien; Guerrero, Josep M.; Vasquez, Juan C.

A Frequency Independent Technique to Estimate Harmonics and Interharmonics in Shipboard Microgrids

Yacine Terriche, *Member, IEEE,* Abderrzak Laib, Abderezak Lashab, *Member, IEEE,* Chun-Lien Su, *Senior Member, IEEE,* Josep M. Guerrero, *Fellow, IEEE,* Juan C. Vasquez, *Senior Member, IEEE*

Abstract— **Modern maritime microgrid systems are witnessing a revolutionary advancement by integrating more renewable energy sources and energy storage systems. The integration of these sophisticated systems is achieved, however, through the power electronics converters that cause severe harmonic contamination. This problem becomes more serious when some of these harmonics that are non-integer multiples of the fundamental (inter-harmonics) exist concurrently with both system frequency drifts and large-power transients, which is a commune issue in maritime microgrid systems such as shipboard microgrids. Hence, the performance of the widely signal processing algorithms applied in the measurement and communication systems such as the smart meters and power quality analyzers tends to worsen. To address this problem this paper proposes an effective method based on the eigenvalue solution to estimate the harmonics and inter-harmonics of modern maritime microgrid systems effectively. This method, which is a system frequency independent technique can work effectively even under large frequency drifts with short window width. The proposed method is evaluated under MATLAB software, and then the experimental validation is carried out via analyzing the electrical power system current of a bulk carrier ship.**

Index Terms— **Fast Fourier transform (FFT), frequency estimation, harmonic assessment, generalized pencil-of-function method (GPOFM), power quality, shipboard power systems, smart maritime microgrids, system frequency-independent technique.**

I. INTRODUCTION

THE substantial trend of the next generation maritime microgrid systems (MMSs) towards self-sufficient systems based on the concept of smart/intelligent grids is increasing vastly [1]. These systems represent an unprecedented opportunity for the MMSs to move towards a green energy era that contributes to efficient, economical, and environmental health technologies [2]. A typical smart system of an AC shipboard microgrid (SMG) is depicted in Fig.1 (a), where the

Y. Terriche, A. Lashab, J. M. Guerrero, and J.C. Vasquez, are with the Department of Energy Technology, Aalborg University, Aalborg 9220, Denmark. (E-mail: yte@et.aau.dk; abl@et.aau.dk; joz@et.aau.dk; juq@et.aau.dk)

A. Laib is with the Departement of Electrical Engineering, University of Jijel, BP 98, Ouled Aissa, Jijel - 18000. (E-mail: abderrzaklaib@yahoo.fr)

C. L. Su is with the Department of Electrical Engineering, National Kaohsiung University of Science and Technology, Kaohsiung, Taiwan. (E-mail: cls@nkust.edu.tw)

structures and mechanisms of the traditional mechanical system are substituted by an all-electrical system based on the power electronic converters (PECs) enabling the integration of renewable energy sources and energy storage systems. The key factors behind these advanced technologies are the utilization of smart appliances and devices such as smart communication and power management systems, smart switches and sensors, intelligent control methods, smart navigation, smart machinery, and smart energy management, etc.[3]. Hence, these technologies are expected to promote several features for the next-generation SMGs such as enhancing power sustainability and system reliability, increasing energy efficiency, and safety [4].

It is facing challenges against the introduction of different types of PECs used in the next-generation MMSs. One of these challenges is the harmonics contamination issue caused by the PECs [5]. The circulation of these harmonics in the electrical power system (EPS) can cause harmful consequences such as inducing the harmonics resonance, creating interferences and malfunctioning of smart communication devices, increasing the losses, misfiring the variable speed drives, affecting the voltage stability, and disturbing the control of the protection equipment [6], [7]. Moreover, the retrofitted and modern ships incorporate the PECs with LCL filters such as the active front ends to control the speed of the thrusters and propellers. These LCL filters create resonance at a certain frequency in interaction with the subtransient reactances of the synchronous generators, transformers, and other passive components. Thus, the power system designers need to ensure that the resonant frequency of the LCL filters does not match the system harmonics. However, if the analyzing algorithm fails to detect any inter-harmonic, in which its frequency matches the resonant frequency of the LCL filters; a significant parallel resonance occurs leading to the augmentation of the current, which conducts to harmonic voltage instability scenarios [8]. If this resonance is not damped it can cause the blackout of the ship and also threatens the lives of the ship crew members/passengers [9]. Practical evidence of the catastrophic accidents of harmonics resonance caused by the LCL filters of PECs occurred in RMS Queen Marry II (QM II) in 2010 [10]. Since then, the maritime industry started paying more attention to harmonics contamination in SMGs. Moreover, precise harmonics analysis of SMGs provides essential information about the level of the distortion to enable the engineers to verify if this distortion respects the power quality standards or requires interference. Furthermore, accurate harmonics analysis helps the engineers to perform
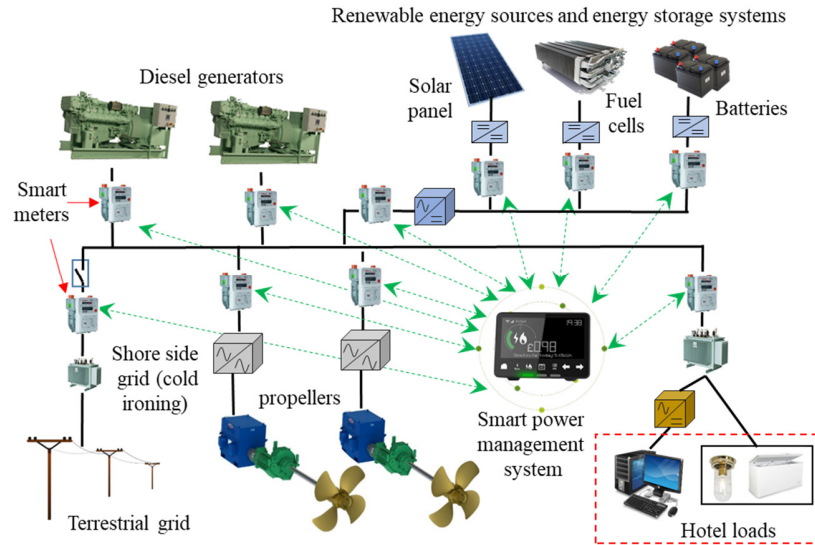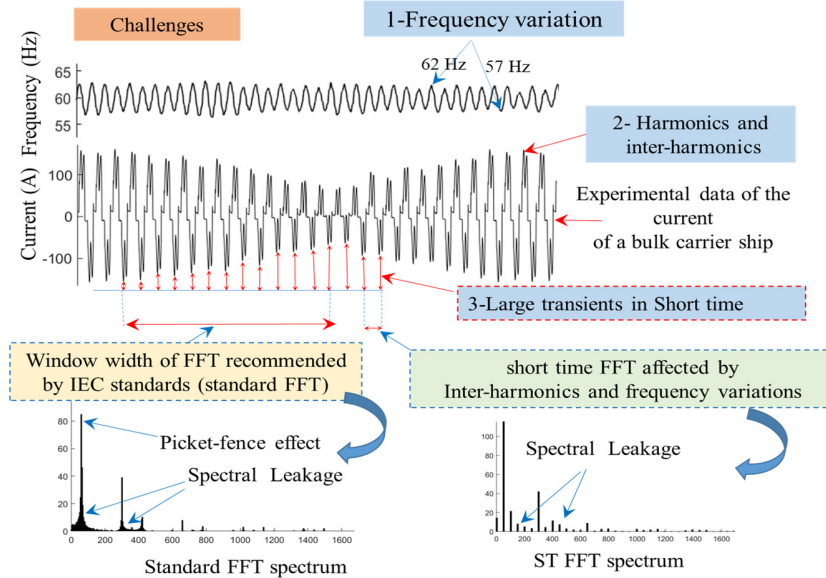
Fig. 1 (a) A generic scheme of smart AC maritime microgrids. (b) Power quality challenges of practical data of a real bulk carrier ship.

comprehension diagnosis including fault detection and location of the synchronous generators and motors [11], [12] and design the appropriate filters taking into account the characteristics and non-characteristic harmonics.

Several techniques have been suggested in the literature to estimate the harmonics/inter-harmonics such as artificial neural networks [13], wavelet packet decomposition [14], fast Fourier transform (FFT) [15], [16], adaptive estimation of the fundamental method [17], Recursive least squares technique [18], Kalman filter (KF) [19], synchronous reference frame (SRF) [20], PQ-theory [21], adaptive cascaded delayed signal cancelation technique [22], [23], real and complex coefficient filters [24], and demodulation of power line signal and subsequent filtering [25]. Nevertheless, none is affirmed to work accurately in inter-harmonic assessment under system

frequency drifts, though each exhibited its benefits. Moreover, most of these techniques are applied to estimate only the fundamentals and require precise information of the system frequency to adapt their moving window as in some cases they require the system phase. Hence, their performance in offline analysis-based short-term protective actions is not possible. The generalized pencil-of-function method (GPOFM) [26], [27] (sometimes referred to as matrix pencil method [28]) is a system frequency independent technique, which means that it does not depend on the signal periodicity to evaluate the harmonics/inter-harmonics of the contaminated data. However, the accuracy of this technique depends on the data-sampling rate. Therefore, the application of the traditional GPOFM in some communication devices cannot be effective, as these devices such as smart meters usually require a low sampling rate due to the limitation of the storage capacity. Furthermore,

another weakness of the traditional GPOFM is the poor average spectral resolution whose frequency bins' maximum rate is decreased down to the half value of the Nyquist–Shannon sampling rate. Therefore, this method did not receive attention in MMS applications or recommendations by related standards. The authors in [29] proposed the interpolation of the data inside the Hankel matrix to increase the eigenvalues, thus, increases the number of the estimated frequencies. However, this method cannot be optimum due to its significant computation burden resulted from performing the singular value decomposition (SVD), eigenvalues calculations, and inverse SVD of the double sized Hankel matrix.

Inspiring by the weakness of the traditional GPOFM, this paper firstly reveals the deficiencies of this traditional GPOFM that have not been discussed before in the literature and demonstrate them mathematically and analytically, then proposes a simple and yet effective method based on virtual exponentials inside the least-square approach to enhance them. Consequently, the proposed method can estimate the harmonics and inter-harmonics accurately with an enhanced resolution under large frequency drifts using a shorter window width. Furthermore, in contradiction with the method proposed in [29], the proposed method can enhance the resolution with a lower computation burden as it does not interpolate any data when performing the SVD and its inverse of the Hankel matrix. In addition, compared to the aforementioned and most applied techniques in literature, the proposed method can estimate the system frequency in an open-loop manner. Hence, it does not require any stability issues or complex controllers design analysis. Therefore, the proposed method is foreseen to be an effective tool for MMSs.

The rest of the paper is organized as follows. In Section II, an overview and problem statement of the traditional GPOFM and FFT is addressed. In section III, the proposed method is detailed. Section IV presents the numerical results and discussions. Section V presents the experimental results and validations. Finally, section VI concludes this paper.

II. Problem Statement

Figure 1 (a) presents a generic single line diagram of next-generation SMG, which dominantly consists of diesel generators, propellers, energy storage systems, hotel loads, and cold ironing. The propellers generally consume about 80% of the total power of the ship during sailing. These propellers are controlled by the voltage frequency drives (VFDs) that cause significant harmonic distortion as shown in Fig. 1 (b). The widely applied technique in signal processing is the FFT due to its simplicity and efficacy of estimating a large number of harmonics up to the aliasing point, as well as the ability to work in offline and online analysis. Hence, most industrial and domestic measurement instruments such as power quality analyzers and smart meters depend on it [15], [16]. Furthermore, the power quality standards often recommend this technique for estimating the harmonics [13], [14]; therefore, this paper considers this technique as a standardized method that merits to be analyzed and compared with the

proposed method for SMGs applications.

What distinguishes the SMGs from terrestrial microgrids are the heavy pulsed loads that consume a large amount of power in a short time. As these ships are usually fed by limited rating synchronous generators, the large demand for power in a short time results in deviating the frequency from its nominal value. Empirical evidence of this assertion is the estimated frequency of the bulk carrier ship in Fig. 1 (b), where it clearly shows that the frequency is constantly fluctuating around the nominal rate. Consequently, the application of the FFT to the experimental data of SMG as shown in Fig. 1 is not suitable and results in spectral leakage, as the FFT is a frequency-dependent technique. For online applications, this issue can be solved by adapting the window size of the FFT using the frequency/phase-locked-loop (FLL/PLL) [30]. However, the FLL/PLL is distinguished by a negative feedback closed-loop system, which can be performed only online; therefore, the application of the FFT in offline analysis-based short-term protective actions becomes a challenge. Some techniques like zero-crossing or maximum crossing methods can be applied to estimate the frequency offline and adapt the FFT [31]. However, the high harmonic distortion, and existance of the inter-harmonics degrade their performance. In addition, the resolution of the short-time FFT (ST-FFT) cannot capture all the harmonics that are non-integer multiples of the fundamental frequency. Hence, if an inter-harmonic appears, the ST-FFT will not be able only to detect it, but also results in the spectral leakage and erroneous information even if its window size matches the periodicity of the signal. The problem becomes more severe when both inter-harmonics and frequency drifts appear together, which is a commune issue in MMSs such as SMGs due to the large variation of the heavy loads in a short time [32]. The application of the windowed interpolated FFT (WI-FFT) using some windows such as Hamming, Hann, and Blackman windows can mitigate the leakage phenomenon [33], [34]. However, as will be demonstrated in the results, this technique divides each harmonic into three bins, one main bin, and two adjacent bins. Hence, under the existence of the inter-harmonics, the adjacent bins will be mixed with the inter-harmonics and cause erroneous information. To address this issue, IEC standards 61000-4-7/30 [35], [36] and the under-revised IEEE 519 standards [37] require the utilization of the FFT with a window size of 10/12 cycles of the fundamental, and the harmonic values are assessed and aggregated within 3-time intervals (three seconds interval, ten minutes interval, and 2 hours interval) [7]. Though these recommendations may reduce the affection of the inter-harmonics, it cannot, however, be a practical solution for SMGs due to the large-signal transient responses caused by the load variations as the FFT can work only for steady-state signals. Hence, the application of both ST-FFT and standard FFT results in the leakage and picket fence effects that degrade their performance as presented in Fig. 1. Though there are several classifications standards for MMSs and rules that cope with harmonics contamination [32], their recommendations are, however, similar to the aforementioned IEC standard. Therefore, there are still many ambiguities and

gaps on how to assess the harmonic distortion of MMSs in the existence of inter-harmonics, frequency drifts, and long transients.

III. RESOLUTION ENHANCEMENT OF GENERALIZED PENCIL OF FUNCTION METHOD

A. Background of the traditional generalized pencil of function method

The GPOFM [26], [27] or sometimes referred to as matrix pencil technique [38]–[40] is a polynomial technique, which factorizes any real or complex signal into a singular value decomposition based on the generalization of the eigendecomposition [28], [39], then, based on the eigenvalue solution, the GPOFM estimates the frequency of each harmonic component [40]. This method is a polynomial technique developed from Prony's method to solve the issue function's interpolation by use of an integral summation of exponentials [39]. Both GPOFM and Prony's methods do not need information about the frequency or the window size when they extract the harmonics. However, the GPOFM features some particular superiorities over Prony's method, which makes it more appropriate for the harmonic and interharmonic estimation. These features are summarized below [28], [29], [38]–[40]:

1. Contrary to Prony's method which is a two-step process that provides the solution in two different steps, the GPOFM is only a one-step process.
2. The GPOFM has a lower variance of the estimated parameters than Prony's method.
3. Contrary to Prony's method, which is proven to be very sensitive to noise, the GPOFM provides better performance in dealing with noise-contaminated signals using the singular value decomposition.
4. In opposed to Prony's method, the GPOFM is not limited to only the aimed frequencies to be estimated and can estimate any harmonic order.
5. The GPOFM has better statistical properties for estimating the frequency components.
6. More precisely, the GPOFM requires less computation burden than Prony's method, which makes it a promising alternative to the discrete Fourier transform with a satisfactory computational burden that enables it to be utilized digitally for power quality analysis applications.

Any perturbed signal can be approximated by a sum of residues and exponentials as [39]:

$$B(kT_s) = \sum_{i=1}^{M} x_i e^{(-\alpha_i + j\omega_i)kT_s} + N(kT_s) \qquad (1)$$

where T_s is the sampling time, k is the step time and expressed as $k = 0,...,\gamma - 1$, γ is the number of samples, x_i are the residues of the complex amplitudes of each frequency i, $N(kT_s)$ is the noise, ω_i is the angular frequency, M is the tolerance, which defines the number of poles to be estimated and introduced as: $i = 1, 2,..,M$, α_i are the damping factors. The execution of the GPOFM begins by selecting a random

window size that is equal or more than a half cycle, then based on the pencil parameter L, the Hankel matrix $[B]$ can be structured, in which each descending skew-diagonal from the right side to the left is fixed as [28]:

$$[B] = \begin{bmatrix} b(1) & b(2) & \dots & b(L+1) \\ b(2) & b(3) & \dots & b(L+2) \\ \vdots & \vdots & \ddots & \vdots \\ b(\gamma - L) & b(\gamma - L + 1) & \dots & b(\gamma) \end{bmatrix}_{(\gamma - L)(L+1)} \qquad (2)$$

In (2), L is referred to as the pencil parameter [26]. In the case of a noisy signal, the GPOFM can offer efficient noise resilience when the parameter L is selected in the interval $\frac{\gamma}{3} \le L \le \frac{\gamma}{2}$ [41]. The singular value decomposition (SVD) of the matrix $[B]$ is expressed as [38]–[40]:

$$[B] = [U][D][V]^T \qquad (3)$$

$$[U] = \begin{bmatrix} U_{1,1} & U_{1,2} & \dots & U_{1,\gamma-L} \\ U_{2,1} & U_{2,2} & \dots & U_{2,\gamma-L} \\ \vdots & \vdots & \ddots & \vdots \\ U_{\gamma-L,1} & U_{\gamma-L,2} & \dots & U_{\gamma-L,\gamma-L} \end{bmatrix}_{(\gamma-L)(\gamma-L)} \qquad (4)$$

$$diag[D] = [\sigma_{1,1}, \sigma_{2,2}...,\sigma(\gamma)]_{(\gamma)} \qquad (5)$$

$$[V] = \begin{bmatrix} V_{1,1} & V_{1,2} & \dots & V_{1,L+1} \\ V_{2,1} & V_{2,2} & \dots & V_{2,L+1} \\ \vdots & \vdots & \ddots & \vdots \\ V_{L+1,1} & V_{L+1,2} & \dots & V_{L+1,L+1} \end{bmatrix}_{(L+1)(L+1)} \qquad (6)$$

where $[U]$ and $[V]$ are orthogonal matrices that contain the eigenvectors of respectively $[[B] \times [B]^T]$ and $[[B]^T \times [B]]$. T denotes the transpose. $[D]$ is a diagonal matrix, which contains the singular positive values σ_i that are the square roots eigenvalues ranked from the most dominant one to the smallest one. The next process is to select the tolerance M, where this choice usually depends on the quality of the signal distortion and sampling time. Hence, the selected σ_i order do not exceed the Shannon-Nyquist frequency, as they become essential noise. Accordingly, for a certain singular value σ_A, some studies select M as [28], [39]:

$$\left(\sigma_A \middle/ \sigma_{max} \right) = 10^p \qquad (7)$$

where p refers to the significant decimal digits of the analyzed data. In case the ratio of the singular values in (7) exceeds p they appear as essential noise. Consequently, selecting M less than that value of (7) results in canceling the noise. After the selection of M, the size of $[V]$ does not match the size of $[D]$ to perform the inverse SVD, thus; the best-fit linear operator to estimate the eigenvalues of the system is performed as:

$$C = pinv([Y_1]) \cdot ([Y_2]) \qquad (8)$$

where $pinv$ denotes the Moore Penrose pseudoinverse of the matrix, $[Y_1]$ and $[Y_2]$ are obtained as:

$$[Y_1] = [U_1][D_1][V_1']^T \qquad (9)$$

$$[Y_2] = [U_1][D_1][V_1'']^T \qquad (10)$$

where $[U_1]$, $[D_1]$, and $[V_1]$ are respectively the reduced matrices of $[U]$, $[D]$, and $[V]$ that are decreased to the selected tolerance M. Accordingly, the exponentials of the distorted signal can be assessed by calculating the eigenvalue solution as:

$$[C] - \lambda_i[I] = 0 \qquad (11)$$

where λ_i are the eigenvalues of each frequency in the distorted data. Then the least square technique to estimate the poles of the harmonics is applied as shown in (12), where $\psi_i = e^{(j\omega_i)T_s}$.

$$
\begin{bmatrix} x_1 \\ x_2 \\ \vdots \\ x_M \end{bmatrix}
=
\begin{bmatrix} A(1) \\ A(2) \\ \vdots \\ A(\gamma) \end{bmatrix}
\bigg\backslash
\begin{bmatrix}
1 & 1 & \cdots & 1 \\
\psi_1 & \psi_2 & \cdots & \psi_M \\
\vdots & \vdots & \ddots & \vdots \\
\psi_1^{\gamma-1} & \psi_2^{\gamma-1} & \cdots & \psi_M^{\gamma-1}
\end{bmatrix}
\qquad (12)
$$

The backslash (\ ) in (12) refers to the least square. One of the main deficiencies in this traditional GPOFM is the small number of harmonics that can be estimated. In the case of factorizing undamped complex signals, the matrix $[D]$ classifies every two rows of σ_i (e.g., $\sigma_{1,1}$ and $\sigma_{2,2}$) for each existent frequency, which implies that the number of frequencies that can be estimated is defined as:

$$f_{max} = (\sigma_{max} / 2) = (L+1)/2 \qquad (13)$$

From (13), one can deduce that the number of frequencies that can be estimated by the GPOFM depends on the parameter L and γ. Fig. 2 presents the maximum number of frequencies that can be extracted by the FFT and GPOFM in terms of the sampling frequency f_s ($f_s = 1/T_s$) and f (f is the frequency, which corresponds to the number of points of γ), where L of the traditional GPOFM is selected in the range of $\gamma/3 \le L \le \gamma/2$. It is obvious that both increasing f_s and the window size result in increasing the number of harmonics that can be estimated by all the methods. Besides, it is clear that the maximum number of the frequency bins that can be estimated by the traditional GPOFM is close to half of those of the FFT when L is set in between $\gamma/3 \le L \le \gamma/2$. Moreover, decreasing L to less than $\gamma/2$ to enhance the noise resilience immunity leads to decreasing the spectral frequency bins. Hence, tends the GPOFM resolution to worsen. In other words, if the number of the characteristic and non-characteristic harmonics that exist in the signal is more than the double number of the estimated eigenvalues in (11), the least square approach performance degrades. This problem becomes more severe when the sampling frequency is relatively low as the resolution and the maximum number of harmonics that can be estimated by the GPOFM is proportional to the switching frequency as presented in Fig. 2 and 3. Interpolating the data inside the Hankel matrix can increase the eigenvalues, thus, increases the number of the estimated frequencies [29]. However, this method cannot be optimum due to its significant computation burden as well as
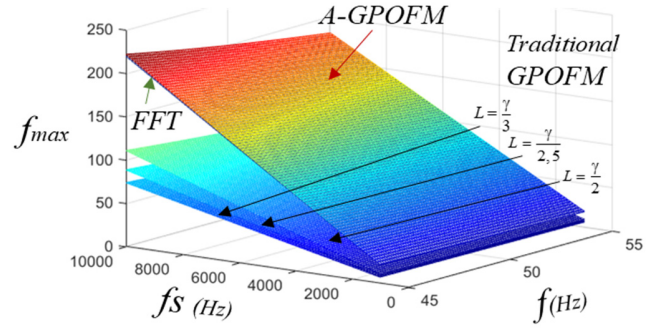

Fig. 2 Maximum number of harmonics can be estimated using the FFT, traditional GPOFM with different values of L, and the AGPOFM in terms of the sampling time and window size.

low performance in the existence of high order harmonics.

B. The proposed method

The GPOFM can be optimized based on the application conditions. For example, in image or voice processing, the fundamental frequency is usually unpredicted. However, for EPSs such as SMGs, the fundamental frequency and its variation limits are predicted (e.g. 60 Hz $\pm$ 2% or 4%). Furthermore, the dominant existed harmonics are the odd harmonics. In some cases, even harmonics and inter harmonics appear with small amplitudes. The main problem occurs when all these harmonics exist under frequency drifts. Hence, traditional methods such as the FFT cannot make distinct whether they are harmonics or inter-harmonics. In addition, the total harmonic distortion (THD) in SMGs is usually calculated with a limited range of harmonics that go up to h_{max} =40 or 50 [32]. This is due to the nature of the harmonics caused by the rectifiers whose amplitude is decreased proportionally with the increase of their frequency order [5]. Empirical evidence of this assertion will be validated in the experimental results. Accordingly, the proposed advanced GPOFM (hereafter called AGPOFM) comprises an effective intern frequency estimator that works in an open-loop pattern. It means that this frequency estimator does have a closed-loop feedback system and does not require any controller design. Hence, it is fully stable and can work effectively for offline analysis. Besides, when the proposed method estimates the frequency of the system, it does not rely on signal periodicity. Consequently, the proposed method does not need a specific window size to analyze the data as long as the number of samples γ is more than half or one cycle. Therefore, this method makes a clear distinction between the harmonics and inter-harmonics even under large frequency drifts. In addition, instead of using the estimated limited number of exponentials using the traditional GPOFM [26], [28], [39] as presented in Fig. 2 to perform the least square solution in (12), the proposed method estimates only the fundamental frequency using the first eigenvalues of (11) that correspond to the dominant singular values of $[D]$. It is noteworthy that the eigenvalues λ_i estimated in (11) are obtained in exponential forms with unitary magnitudes as:

$$\lambda_i = [e^{(-\alpha_1+j\omega_1)kT_s}, e^{(-\alpha_1+j\omega_1)kT_s}, e^{(-\alpha_2+j\omega_2)kT_s},$$

$$e^{(-\alpha_2+j\omega_2)kT_s}, \ldots e^{(-\alpha_M+j\omega_M)kT_s}, e^{(-\alpha_M+j\omega_M)kT_s}] \qquad (14)$$

simplified to:

$$\hat{f} = \frac{f_s \omega_1 T_s}{2\pi} \tag{17}$$

As the sampling frequency is the average number of samples obtained in one second ($f_s = 1/T_s$), the multiplication of f_s and T_s results in one. Thus, (17) becomes:

$$\hat{f} = \frac{\omega_1}{2\pi} \tag{18}$$

After estimating the fundamental frequency, the proposed method creates virtual exponentials tuned at the odd and even harmonics up to h_{max} as well as at the adjacent inter-harmonics between every two harmonics as presented in (19) to perform the least square solution. Where the vectors $[x]$ and $[A]$ refer to the poles (harmonics amplitudes) and the contaminated data, respectively, and $[E]$ is the matrix of the virtual exponentials. Consequently, the maximum number of harmonics using the proposed method is improved up to the aliasing point as presented in Fig. 2. It is noteworthy that the virtual exponentials in (19) are adapted with the intern frequency estimator $\hat{f}$ during the estimation of the poles. Therefore, neither the frequency drifts nor the window size variation can affect its performance. Furthermore, the number of inter-harmonics between every two harmonics in (19) is 9 (e.g., the virtual inter-harmonics between the harmonics $h=2$ and $h=3$ are $e^{kj2\pi\hat{f}T_s2}, e^{kj2\pi\hat{f}T_s2.1}, e^{kj2\pi\hat{f}T_s2.2}, ..., e^{j2\pi\hat{f}T_s3}$). Increasing the number of the virtual inter-harmonics between every two

harmonics (e.g. $e^{kj2\pi\hat{f}T_s2}, e^{kj2\pi\hat{f}T_s2.05}, e^{kj2\pi\hat{f}T_s2.1}, ..., e^{j2\pi\hat{f}T_s3}$) results in further resolution enhancement. However, the excessive increase results in elevating the computation burden. It is noteworthy that α_i are neglected for the sake of simplicity as the size of the moving window proposed method is very short (1 cycle). As long as the matrix $[A]$ is not square, the solution to (19) is achieved as formulated in (20).

$$[x] = Pinv([E])[A] \tag{20}$$

The Moore Penrose pseudoinverse of $[E]$ in (20) can be calculated in different ways, one of the most effective ways is to use the SVD as:

$$[E] = [U_e][D_e][V_e]^T \tag{21}$$

$$Pinv([E]) = [V_e][D_e]^{-1}[U_e]^T \tag{22}$$

where the descriptions of $[U_e]$, $[D_e]$, and $[V_e]$ are the same of $[U]$ $[D]$ $[V]$ in (3). The superscript (-1) refers to the matrix inverse.

The spectral resolution of the GPOFM is different from the one of the FFT as the resolution of the FFT is only proportional to the window width and expressed as:

$$\text{Re}\,s_{FFT} = f_s / \gamma \tag{23}$$

The traditional GPOFM, on the other hand, can estimate any inter-harmonic of the contaminated data. However, the maximum number of the estimated frequencies is confined in the range $\gamma/6 \le f_{max} \le \gamma/4$. Therefore, unfortunately, no linear-equation can represent the resolution of the GPOFM as it is variable. Accordingly, the spectral resolution of the GPOFM can be effectively evaluated in this paper by estimating the average difference of the frequency bins to visualize the sampling time and window size influence as:

$$\text{Re}\,s_{GPOFM} = f_s / L, \qquad L \in [\gamma/3 \; \gamma/2] \tag{24}$$

On the other hand, conversely to the aforementioned methods, the resolution of the proposed AGPOFM is proportional to the virtual harmonics and inter-harmonics applied in the matrix $[E]$ to perform the least square approach and to the moving window size as presented in (25).

$$\text{Re}\,s_{AGPOFM} = f_s / (\gamma \cdot P) \tag{25}$$

where P is the number of the virtual inter-harmonics between every two harmonics. The larger P is the better resolution is. Better visualizing of the resolution is presented in Fig. 3, where it is evident that the FFT resolution is only proportional to the size of the window, and remains fixed during the sampling time variation. However, the traditional GPOFM resolution is significantly influenced by both window size and the sampling

$$\begin{bmatrix} x_1 \\ x_{1.1} \\ \vdots \\ x_2 \\ \vdots \\ x_{h_{max}} \end{bmatrix} = \begin{bmatrix} A(1) \\ A(2) \\ \vdots \\ A(\gamma) \end{bmatrix} \backslash \begin{bmatrix} 1 & 1 & \cdots & 1 & \cdots & 1 \\ e^{1(j2\pi\hat{f}1T_s)} & e^{1(j2\pi\hat{f}1.1T_s)_s} & \cdots & e^{1(j2\pi\hat{f}2T_s)} & \cdots & e^{1(j2\pi\hat{f}h_{max}T_s)} \\ e^{2(j2\pi\hat{f}1T_s)} & e^{2(j2\pi\hat{f}1.1T_s)} & \cdots & e^{2(j2\pi\hat{f}2T_s)} & \cdots & e^{2(j2\pi\hat{f}h_{max}T_s)} \\ \vdots & \vdots & \ddots & \vdots & \ddots & \vdots \\ e^{\gamma(j2\pi\hat{f}1T_s)} & e^{\gamma(j2\pi\hat{f}1.1T_s)} & \cdots & e^{\gamma(j2\pi\hat{f}2T_s)} & \cdots & e^{\gamma(j2\pi\hat{f}h_{max}T_s)} \end{bmatrix} \tag{19}$$
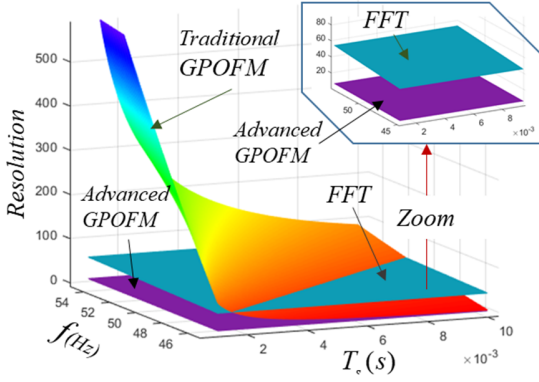
Fig. 3 The spectral resolution of the traditional GPOFM, the FFT and the advanced GPOFM in terms of the sampling time and window size.

time. Hence, at a certain window size and sampling frequency, its average resolution becomes better than the FFT. It is noteworthy that the smaller the resolution is the better accuracy is. On the other hand, the resolution of the proposed method is significantly improved by increasing the number of virtual exponentials. In this paper, it will be demonstrated that in the case of analyzing the data of an SMG, setting P is set to 9 (see Eq.(19)) can provide sufficient accuracy. The choice of selection P=9 is preferred to follow the IEC Standard 61000-4-7/30 requirements regarding the number of aimed interharmonics between every two harmonics.

IV. NUMERICAL RESULTS AND DISCUSSIONS

The simulation results are carried out under MATLAB software. Fig. 4 shows the performance of the traditional GPOFM, the ST-FFT, the standard FFT, WI-FFT, and the proposed method in estimating the harmonic distortion of a distorted signal. T_s is set to 2e-4, the frequency of the system is 50 Hz, which changes to 52 Hz after 1250 samples. The first subplot presents the signal, which is contaminated with low-order and high-order harmonics and some inter-harmonics. The second subplot presents the efficacy of the proposed method in estimating the fundamental frequency of the signal using (15), where it is evident that when the frequency drifts from 50 to 52 Hz, the proposed method accurately estimates the frequency variation with a fast transient response (one cycle) even under the existence of the inter-harmonics. It is noteworthy that the ST-FFT, standard FFT, and the WI-FFT are frequency-dependent methods that cannot estimate the frequency, while the traditional GPOFM fails to estimate the system frequency under high distortion and poor sampling time. Therefore, only the frequency estimated by the proposed method is presented. Besides, for the sake of clarity, the THD of these methods is plotted in two subplots using the following equations:

$$THD = \frac{\sqrt{\sum_{h=2}^{n} B_h^2}}{B_1} \cdot 100 \qquad (26)$$

where B_1 and B_h are respectively the RMS values of the fundamental and harmonics components. h refers to the harmonic order. n represents the number of harmonics, which is according to the most leading classification societies, it is selected up to 50th order (or o 100th if the active front ends are
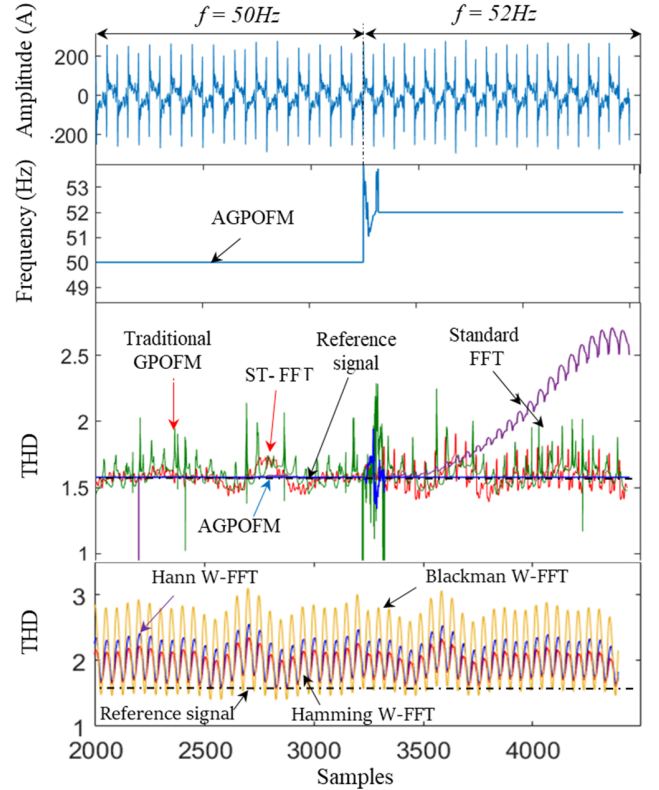

Fig. 4 Performance of the proposed AGPOFM, traditional GPOFM, ST-FFT, standard FFT, and WI-FFT to assess the harmonic distortion under frequency drifts.

used) [5]. According to the third subplot of Fig. 4, the ST-FFT provides a fast transient response, its accuracy tends, however, to worsen due to the existence of inter-harmonics. Moreover, the frequency drift leads to further accuracy degradation of the SF-FFT, which can be visualized in the harmonic spectrum of Fig. 5, range number 2 that does not match the reference harmonics due to the spectral leakage and picket-fence effect. The standard FFT can provide accurate THD estimating even in the existence of inter-harmonics. However, its transient response under frequency drifts is very long that increases the spectral leakage as demonstrated in Fig. 5, range number 3. The traditional GPOFM can work properly if the value of f_s is high and the signal has a low number of harmonics. However, due to the low value of f_s (f_s =2.5 kHz) and the high number of harmonics, the performance of the traditional GPOFM tends to worsen. Hence, results in wrong information as shown in Fig. 5, range number 4. On the other hand, the proposed AGPOFM can estimate the THD by following the reference signal accurately with a faster transient response (one cycle) under frequency drifts. Furthermore, according to Fig. 5, range number 5, it is obvious that the proposed method can estimate the harmonics and inter-harmonics accurately that matches the reference ones in range number 1. The last subplot of Fig. 4 presents the performance of the WI-FFT based on Hamming, Hann, and Blackman windows, where it is clear that these methods are not suitable when using a window size of one cycle. Hence, they result in a lot of fluctuations and erroneous information. Furthermore, the ranges 6, 7, and 8 of the harmonic spectrum of Fig. 5 show that these methods
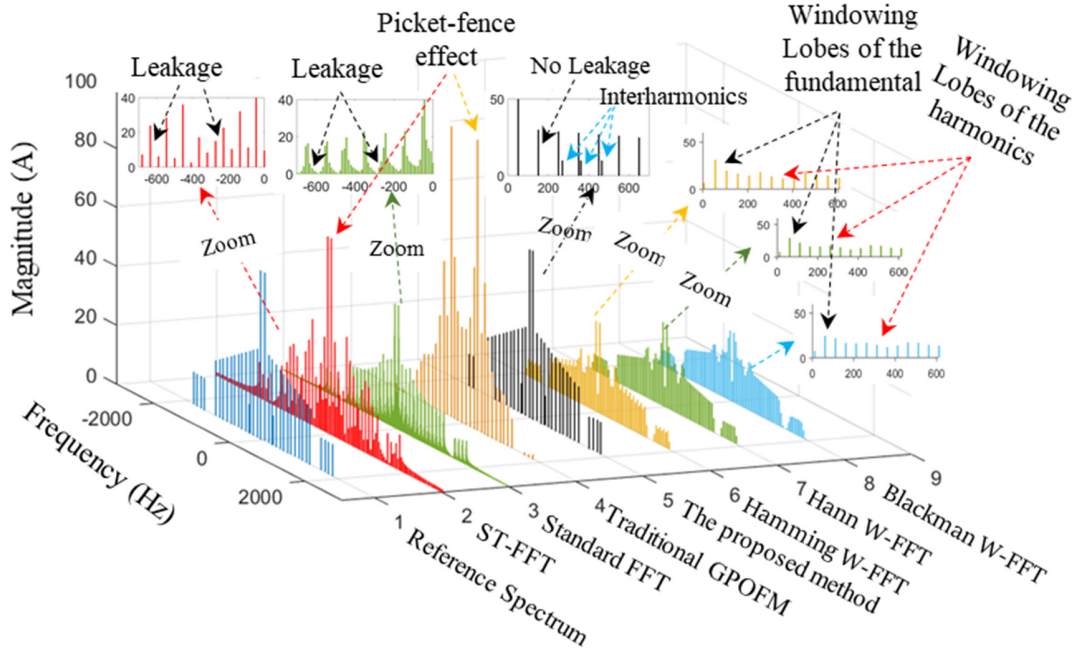
Fig. 5 Harmonic spectrum extracted by the proposed AGPOFM, traditional GPOFM, ST-FFT, standard FFT, and WI-FFT.

succeeded decreasing the leakage. however, since the hypothesis of these methods is to factorize each bin into 3 bins, where two of them are adjacent to the main one results in confusion with the inter-harmonics when the resolution of the sampled data is weak.

V. EXPERIMENTAL RESULTS AND DISCUSSIONS

For the experimental verification of the proposed method, a bulk carrier ship, which is presented in Fig. 6 (a) is selected. Since this type of ship is designed to lift and transport unpackaged bulk cargo, the measurements were carried out during the operation of the windlass, and the mooring winches. The data is collected using Hioki 8847 Memory HiCorder presented. The sensors of the measurement devices are connected to the main switchboard of the electrical power system as shown in Fig. 6(b). The essential parameters of the EPS of this ship are summarized in Table. I.

Figure 7 presents the performance of the traditional GPOFM, the ST-FFT, the standard FFT, WI-FFT, and the proposed method in estimating the THD. The first subplot depicts the experimentally contaminated current that has large transients
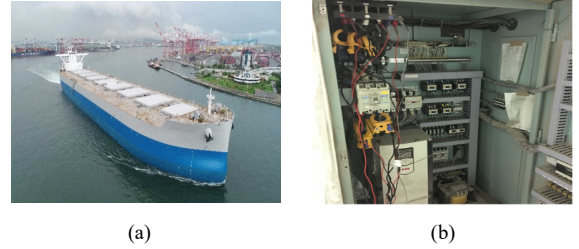

(a)   (b)

Fig. 6 Electrical power system of a bulk carrier ship. (a) Picture of the selected bulk carrier ship. (b) Sensors of the measurement devices that are connected to the main switchboard of the electrical power system.

Fig. 7 Experimental results of the proposed AGPOFM, traditional GPOFM, ST-FFT, standard FFT, and WI-FFT on assessing the current harmonic distortion of a bulk carrier ship.

TABLE I
SHIPBOARD POWER SYSTEM PARAMETERS

Items and Equipment	Parameters	Values
Main AC bus voltage	Vabc[Vrms]	440V
	f [Hz]	60Hz
Diesel generator (3sets)	Vg[Vrms]	450V
	Pg[kW]	950kW
	Xd'[%]	28.4
	Xd''[%]	15.3
	Cos(ψg)	0.8
Windlass & mooring winch	Vm[Vrms]	440V
(8 sets)	Pm[kW]	60kW
Main engine	Pm[kW]	11920kW
Fuel tank	Weight[t]	396 tons
Speed	Knots	14.5 Knots

due to the load variation. Similar to the simulation results, it is clear that the ST-FFT struggles from lots of oscillations caused by the frequency drifts, which results in the spectral leakage as presented in Fig. 8(a). Though the standard FFT can overcome the weakness of the oscillations caused by frequency drifts in estimating the THD, its transient response is, however, very long during the load variation, which results in incorrect information. This can be clear in Fig. 8(b) where the associated arrows that show the maximum and minimum load variation become vertical due to the delay compared with the other spectrums. Furthermore, the large window size of the standard FFT does not provide accurate THD information under short variations of the load as shown in Fig. 7, where it missed the

information of a 20 % increase of the real THD. As the sampling time is high and the distortion is high, the traditional GPOFM fails to estimate the THD resulting in large oscillations caused by the erroneous information that appears in the THD subplot of Fig. 7 and erroneous bins in the harmonic spectrum of Fig. 8(c). The WI-FFT based on Hamming, Hann, and Blackman windows succeeded minimizing the leakage as depicted in Fig. 8 (d) and (e) (the spectrum of WI-FFT based on Blackman window is not plotted as it has similar behavior to Hamming and Hann windows). However, these methods create adjacent bins extracted from the existent bins, which make confusion with the inter-harmonics. Furthermore, measuring the THD using these methods with a short window is not
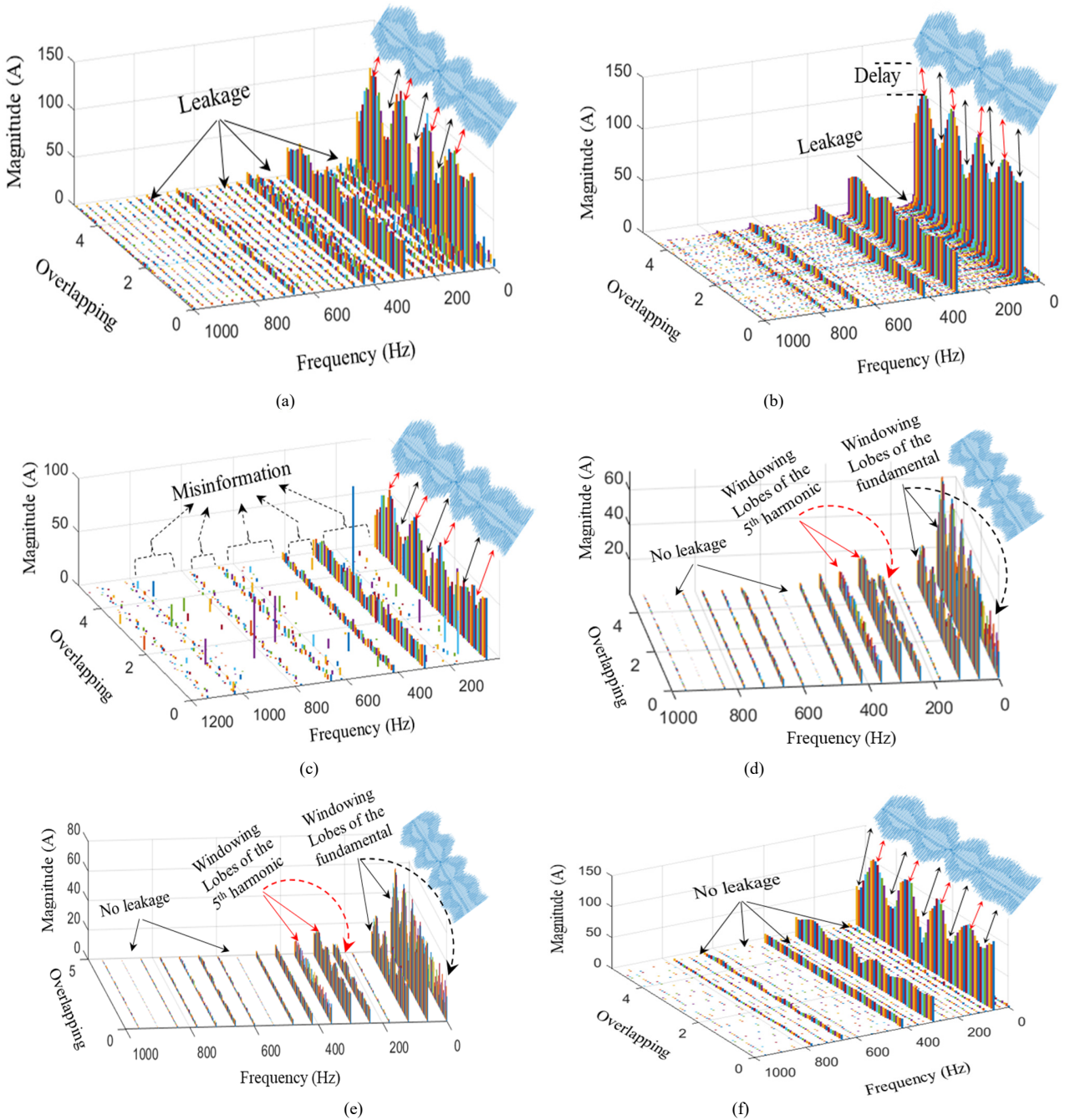

Fig. 8 Experimental results of 3D harmonic spectrums estimated by: (a) the ST-FFT. (b) the standard FFT. (c) the traditional GPOFM. (d) WI-FFT based on Hamming window. (e) WI-FFT based on Hann window. (f) the proposed AGPOFM

efficient as they result in significant fluctuations and erroneous information as demonstrated in the last subplot of Fig. 7. However, the proposed method suffers neither from the fluctuations caused by the frequency drifts nor from the leakage as presented in Fig. 8 (f). In addition, the proposed method provides an accurate THD estimation with a very fast transient response during the load variation as presented in Fig. 7. Besides, the proposed method can estimate the system frequency with an open-loop pattern as shown in the last subplot of Fig.7. Hence, this method is unconditionally stable and does not need any controller designs or stability analysis.

Figure 9 presents the computation burden of the proposed method and the enhanced sliding matrix pencil method (SMPM) proposed in [29]. The number of virtual exponentials between every two harmonics in the proposed method is set to 9 (P in (25) is set to 9) to provide a satisfactory interharmonics assessment. From the mathematical development of the SMPM, it is obvious that creating interpolating poles between each two harmonics to enhance the resolution results in enlarging the Hankel Matrix to a double size. Consequently, the computation burden of all the rest equations including the SVD and the least square significantly increases. However, though the proposed method achieves resolution that is more efficient than the SMPM, it only increases the computation of (19) based on the virtual exponentials, as the size of the Hankel matrix does not increase and all rest equations will compute lower size matrices. A very effective technique to compare the computation burden of both algorithms is by executing the same data under the same conditions and use a program that evaluates the elapsed time. As the computation burden varies depending on the processor of the computer, in this study case, Intel(R) Core (TM) i5-8250U CPU @ 1.60 GHz processor with a RAM of 8 GB is utilized. Though in this study case the resolution of the proposed method is better than the one of the SMPM, the elapsed time of the proposed method is very small compared to the SMPM, which implies that the proposed method has a more effective computation burden. It is noteworthy that this elapsed time can effectively vary based on the resolution (selection of P in (25)) that fits the signal type. As the values of the non-characteristic harmonics are usually small in SMGs due to the nature of the three-phase nonlinear loads, keeping P selected to 9 in the proposed method is very efficient to provide accurate harmonics analysis.
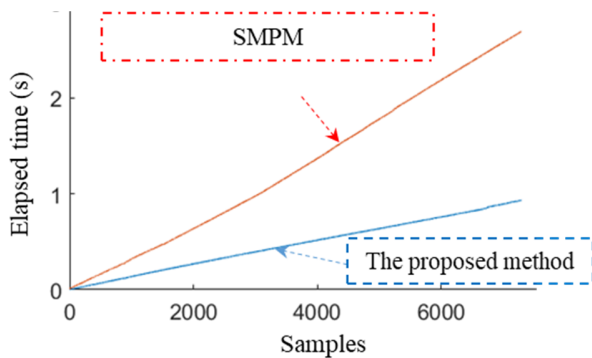

Fig. 9 Computation burden of the proposed method and SMPM

VI.   . CONCLUSIONS

In this paper, a system frequency independent technique is proposed to estimate the harmonics and inter-harmonics of smart MMSs by solving the eigenvalue problem. The evaluation of the proposed method is carried out under MATLAB software and validated experimentally by analyzing the current of a bulk carrier ship during the operation of the mooring winches and the windlass. Based on the conducted work, several features have been achieved such as:

- Ability to assess a wider range of harmonics as its resolution is enhanced by the proposed virtual exponentials tuned at the aimed harmonics and inter-harmonics. Consequently, the proposed method can effectively enhance the resolution and increase the maximum number of the spectral frequency bins up to the Nyquist-Shannon sampling frequency.
- Signal periodicity independent characteristic (the variation of the window size of the analyzed data does not affect its accuracy)
- System frequency-independent feature (it does not rely on any other frequency estimators as it has an intern frequency estimator that works in an open-loop pattern. Hence, its stability is unconditional and does not require any controllers design or stability analysis)
- Capability to work effectively under a low sampling rate.

Besides, based on the obtained results, the calculated THD is found to be very serious (varies from 43%-80%) according to the IEC61000-3-6 and IEEE Std 519TM-2014 standards. Hence, installing sophisticated filters is necessary to avoid the dangerous consequences that may lead to the blackout of the ship.

REFERENCES

[1] T. R. B. Kushal, K. Lai, and M. S. Illindala, "Risk-based Mitigation of Load Curtailment Cyber Attack Using Intelligent Agents in a Shipboard Power System," *IEEE Trans. Smart Grid*, Aug. 2018.

[2] B. Weinert, M. Uslar, and A. Hahn, "System-of-systems: How the maritime domain can leam from the Smart Grid," in *Proceedings Elmar - International Symposium Electronics in Marine*, 2017, vol. 2017-September, pp. 229–232.

[3] S. Fang, Y. Wang, B. Gou, and Y. Xu, "Toward Future Green Maritime Transportation: An Overview of Seaport Microgrids and All-Electric Ships," *IEEE Transactions on Vehicular Technology*, vol. 69, no. 1. Institute of Electrical and Electronics Engineers Inc., pp. 207–219, 01-Jan-2020.

[4] Y. L. Tang and N. N. Shao, "Design and research of integrated information platform for smart ship," in *2017 4th International Conference on Transportation Information and Safety, ICTIS 2017 - Proceedings*, 2017, pp. 37–41.

[5] Control of Harmonics in Electrical Power Systems, American Bureau of Shipping Guidance, 2006

[6] C. I. Chen, Y. C. Chen, Y. C. Chin, and C. H. Chen, "Integrated power-quality monitoring mechanism for microgrid," *IEEE Trans. Smart Grid*, vol. 9, no. 6, pp. 6877–6885, Nov. 2018.

[7] A. Micallef, M. Apap, C. Spiteri-Staines, and J. M. Guerrero, "Mitigation of Harmonics in Grid-Connected and Islanded Microgrids Via Virtual Admittances and Impedances," *IEEE Trans. Smart Grid*, pp. 1–11, 2015, doi.

[8] H. Hu, Q. Shi, Z. He, J. He, and S. Gao, "Potential harmonic resonance impacts of PV inverter filters on distribution systems," *IEEE Trans. Sustain. Energy*, vol. 6, no. 1, pp. 151–161, Jan. 2015.

[9] Y. Terriche *et al.*, "A Hybrid Compensator Configuration for VAR Control and Harmonic Suppression in All-Electric Shipboard Power Systems," *IEEE Trans. Power Deliv.*, pp. 1–1, 2019.

[10] R. M. S. Q. Mary, "RMS Queen Mary 2 Report No 28/2011.," no. 28, 2011.

[11] J. Li, Q. Yang, H. Mu, S. Le Blond, and H. He, "A new fault detection and fault location method for multi-terminal high voltage direct current of offshore wind farm," *Appl. Energy*, vol. 220, pp. 13–20, Jun. 2018.

[12] M. A. Moussa, M. Boucherma, and A. Khezzar, "A Detection Method for Induction Motor Bar Fault Using Sidelobes Leakage Phenomenon of the Sliding Discrete Fourier Transform," *IEEE Trans. Power Electron.*, vol. 32, no. 7, pp. 5560–5572, Jul. 2017.

[13] L. L. Lai, W. L. Chan, C. T. Tse, and A. T. P. So, "Real-time frequency and harmonic evaluation using artificial neural networks," *IEEE Trans. Power Deliv.*, vol. 14, no. 1, pp. 52–59.

[14] L. Eren, M. Unal, and M. J. Devaney, "Harmonic Analysis Via Wavelet Packet Decomposition Using Special Elliptic Half-Band Filters," *IEEE Trans. Instrum. Meas.*, vol. 56, no. 6, pp. 2289–2293, Dec. 2007.

[15] W. Zhou, O. Ardakanian, H. T. Zhang, and Y. Yuan, "Bayesian Learning-Based Harmonic State Estimation in Distribution Systems with Smart Meter and DPMU Data," *IEEE Trans. Smart Grid*, vol. 11, no. 1, pp. 832–845, Jan. 2020.

[16] B. Subhash and V. Rajagopal, "Overview of smart metering system in Smart Grid scenario," in *2014 Power and Energy Systems Conference: Towards Sustainable Energy, PESTSE 2014*, 2014.

[17] D. M. McNamara, A. K. Ziarani, and T. H. Ortmeyer, "A New Technique of Measurement of Nonstationary Harmonics," *IEEE Trans. Power Deliv.*, vol. 22, no. 1, pp. 387–395, Jan. 2007.

[18] A. El Zawawi, K. H. Youssef, and O. A. Sebakhy, "Recursive least squares Harmonic identification in active power filters," in *2007 European Control Conference (ECC)*, 2007, pp. 4645–4650.

[19] X. Nie, "Detection of Grid Voltage Fundamental and Harmonic Components Using Kalman Filter Based on Dynamic Tracking Model," *IEEE Trans. Ind. Electron.*, pp. 1–1, 2019.

[20] D. Campos-Gaona, R. Pena-Alzola, J. L. Monroy-Morales, M. Ordonez, O. Anaya-Lara, and W. E. Leithead, "Fast selective harmonic mitigation in multifunctional inverters using internal model controllers and synchronous reference frames," *IEEE Trans. Ind. Electron.*, vol. 64, no. 8, pp. 6338–6349, Aug. 2017.

[21] A. Rachid *et al.*, "PQ Theory-Based Control of Single-Stage V2G Three-Phase BEV Charger for High-Voltage Battery," in *IFAC-PapersOnLine*, 2019, vol. 52, no. 29, pp. 73–78.

[22] S. Golestan, M. Ramezani, J. M. Guerrero, and M. Monfared, "dq-Frame Cascaded Delayed Signal Cancellation- Based PLL: Analysis, Design, and Comparison With Moving Average Filter-Based PLL," *IEEE Trans. Power Electron.*, vol. 30, no. 3, pp. 1618–1632, Mar. 2015.

[23] Y. Terriche *et al.*, "Adaptive CDSC-Based Open-Loop Synchronization Technique for Dynamic Response Enhancement of Active Power Filters," *IEEE Access*, vol. 7, pp. 96743–96752, 2019.

[24] Y. Terriche, S. Golestan, J. M. Guerrero, and J. C. Vasquez, "Multiple-Complex Coefficient-Filter-Based PLL for Improving the Performance of Shunt Active Power Filter under Adverse Grid Conditions," in *IEEE Power and Energy Society General Meeting*, 2018, vol. 2018-August.

[25] C. A. G. Marques, M. V. Ribeiro, C. A. Duque, P. F. Ribeiro, and E. A. B. Da Silva, "A controlled filtering method for estimating harmonics of off-nominal frequencies," *IEEE Trans. Smart Grid*, vol. 3, no. 1, pp. 38–49, Mar. 2012.

[26] Y. Hua and T. K. Sarkar, "Generalized pencil-of-function method for extracting poles of an EM system from its transient response," *IEEE Trans. Antennas Propag.*, vol. 37, no. 2, pp. 229–234, Feb. 1989.

[27] B. Yektakhah and K. Sarabandi, "All-directions through the wall radar imaging enhancement using orthogonal polarizations and generalized pencil of function method," in *IEEE Antennas and Propagation Society, AP-S International Symposium (Digest)*, 2015, vol. 2015-October, pp. 695–696.

[28] K. Sheshyekani, G. Fallahi, M. Hamzeh, and M. Kheradmandi, "A General Noise-Resilient Technique Based on the Matrix Pencil Method for the Assessment of Harmonics and Interharmonics in Power Systems," *IEEE Trans. Power Deliv.*, vol. 32, no. 5, pp. 2179–2188, Oct. 2017.

[29] Y. Terriche *et al.*, "A Resolution-Enhanced Sliding Matrix Pencil Method for Evaluation of Harmonics Distortion in Shipboard Microgrids," *IEEE Trans. Transp. Electrif.*, vol. 6, no. 3, pp. 1290–1300, Sep. 2020.

[30] S. Golestan, J. M. Guerrero, and J. Vasquez, "Modeling and Stability Assessment of Single-Phase Grid Synchronization Techniques: Linear Time-Periodic vs. Linear Time-Invariant Frameworks," *IEEE Trans. Power Electron.*, vol. 8993, no. c, 2018.

[31] M. B. Durić and Ž. R. Durišić, "Frequency measurement in power networks in the presence of harmonics using fourier and zero crossing technique," in *2005 IEEE Russia Power Tech, PowerTech*, 2005.

[32] J. Mindykowski, "Case Study—Based Overview of Some Contemporary Challenges to Power Quality in Ship Systems," *Inventions*, vol. 1, no. 4, p. 12, 2016.

[33] C. Luo, X. Xu, M. An, L. Mao, and W. Zhou, "Research and Design of Data Acquisition and Processing Algorithm Based on Improved FFT," in *Proceedings of the 31st Chinese Control and Decision Conference, CCDC 2019*, 2019, pp. 1599–1604.

[34] Sulistyaningsih, P. Putranto, P. Daud, and W. Desvasari, "Fast Fourier Transform (FFT) Data Sampling using Hamming and Blackman Method for Radar," in *Proceedings of 2018 International Conference on Electrical Engineering and Computer Science, ICECOS 2018*, 2019, pp. 183–188.

[35] IEC61000-4-15 -2010-08 - (EMC) – Part 4-15: Testing and measurement techniques – Flickermeter – Functional and design specifications.

[36] IEEE P1668/D4Q, May 2014 : IEEE Approved Draft Recommended Practice for Voltage Sag and Interruption Ride-Through Testing for End Use Electrical Equipment Less than 1,000 Volts. IEEE, 2014.

[37] *IW Group, 2014. 519-2014-IEEE Recommended Practice and Requirements for Harmonic Control in Electric Power Systems. IEEE Std 519–2014 (Revision of IEEE Std 519–1992), pp.1-29*

[38] R. S. Adve, T. K. Sarkar, O. M. C. Pereira-Filho, and S. M. Rao, "Extrapolation of time-domain responses from three-dimensional conducting objects utilizing the matrix pencil technique," *IEEE Trans. Antennas Propag.*, vol. 45, no. 1, pp. 147–156, 1997.

[39] T. K. Sarkar and O. Pereira, "Using the matrix pencil method to estimate the parameters of a sum of complex exponentials," *IEEE Antennas Propag. Mag.*, vol. 37, no. 1, pp. 48–55, Feb. 1995.

[40] N. Yilmazer, Jinhwan Koh, and T. K. Sarkar, "Utilization of a unitary transform for efficient computation in the matrix pencil method to find the direction of arrival," *IEEE Trans. Antennas Propag.*, vol. 54, no. 1, pp. 175–181, Jan. 2006.

[41] Y. Hua and T. K. Sarkar, "On the total least squares linear prediction method for frequency estimation," *IEEE Trans. Acoust.*, vol. 38, no. 12, pp. 2186–2189, Dec. 1990.